molecular pharmaceutics

Article

Cite This: Mol. Pharmaceutics 2019, 16, 2494−2501

pubs.acs.org/molecularpharmaceutics

An Integrated Microfluidic Platform for Quantifying Drug Permeation across Biomimetic Vesicle Membranes

Michael Schaich,[†] Jehangir Cama,[†,‡] Kareem Al Nahas,[†] Diana Sobota,[†] Hannah Sleath,[†] Kevin Jahnke,[†,§,∥] Siddharth Deshpande,[⊥] Cees Dekker,[⊥] and Ulrich F. Keyser*[,†]

[†]Cavendish Laboratory, University of Cambridge, JJ Thomson Avenue, Cambridge CB3 0HE, U.K.

[‡]Living Systems Institute, University of Exeter, Stocker Road, Exeter EX4 4QD, U.K.

[§]Department of Biophysical Chemistry, University of Heidelberg, Im Neuenheimer Feld 253, D-69120 Heidelberg, Germany

[∥]Department of Cellular Biophysics, Max Planck Institute for Medical Research, Jahnstraße 29, D-69120 Heidelberg, Germany

[⊥]Department of Bionanoscience, Kavli Institute of Nanoscience, Delft University of Technology, Van der Maasweg 9, 2629 HZ Delft, The Netherlands

Supporting Information

ABSTRACT: The low membrane permeability of candidate drug molecules is a major challenge in drug development, and insufficient permeability is one reason for the failure of antibiotic treatment against bacteria. Quantifying drug transport across specific pathways in living systems is challenging because one typically lacks knowledge of the exact lipidome and proteome of the individual cells under investigation. Here, we quantify drug permeability across biomimetic liposome membranes, with comprehensive control over membrane composition. We integrate the microfluidic octanol-assisted liposome assembly platform with an optofluidic transport assay to create a complete microfluidic total analysis system for quantifying drug permeability. Our system enables us to form liposomes with charged lipids mimicking the negative charge of bacterial membranes at physiological pH and salt concentrations, which proved difficult with previous liposome formation techniques. Furthermore, the microfluidic technique yields an order of magnitude more liposomes per experiment than previous assays. We demonstrate the feasibility of the assay by determining the permeability coefficient of norfloxacin and ciprofloxacin across biomimetic liposomes.

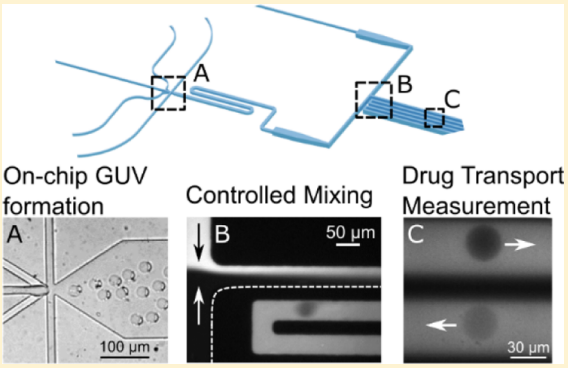

KEYWORDS: *microfluidics, lab on chip, liposomes, GUV, antibiotics, drug transport, permeability*

1. INTRODUCTION

Over the past decades, multidrug resistance in microbial pathogens has developed into a serious threat for public health, leading to a global medical crisis.[1] In 2016, more than half (58.6%) of clinical *Escherichia coli* isolates in the European Union showed resistance to at least one of the antimicrobial groups under regular surveillance.[2] One of the major biochemical causes of antibiotic resistance is the reduced membrane permeability of drug molecules.[3−6] This problem is especially apparent for Gram-negative bacteria, as their cell envelope consists of a double membrane; drugs require seemingly contradictory chemical properties to overcome these two barriers to reach their cytoplasmic targets.[4,6,7] A deeper understanding of the mechanisms that govern passive drug transport across lipid membranes is therefore of great importance.

Bacterial cell membranes are very complex systems that are involved in numerous cellular processes.[8] Drug permeability studies have proven very difficult not only because of the small size of the bacteria but also because of the convolution of active and passive effects that simultaneously take place in the membranes of living bacteria.[6,9] Many studies on membrane properties are therefore performed using lipid vesicles (or liposomes) as model systems.[9] Liposomes of several microns in size, referred to as giant unilamellar vesicles (GUVs), offer the advantages of having well-defined lipid compositions, being easy to image and also being more controlled systems for studying transport processes than a living bacterium. Because of these advantages, liposomes have been the subject of intensive research and their applications now reach far beyond the drug delivery[10] and synthetic biology communities.[11−13]

Various methods to produce lipid vesicles have been developed.[14] Albeit offering good control over lipid composition, many technologies such as electroformation suffer from drawbacks such as low yield, batch-to-batch variability, low

Received: January 18, 2019
Revised: March 21, 2019
Accepted: April 17, 2019
Published: April 17, 2019

DOI: 10.1021/acs.molpharmaceut.9b00086
Mol. Pharmaceutics 2019, 16, 2494−2501

encapsulation efficiency, and polydispersity; these problems are especially acute at high salt concentrations and when using charged lipids.[15] Microfluidic methods to form liposomes can overcome these limitations but often require oil as the lipid-carrying solvent, which must be removed in further procedures.[16] The recently developed microfluidic technique octanol-assisted liposome assembly (OLA) replaces the oil phase with the aliphatic alcohol 1-octanol.[17] A double emulsion of water in octanol self-assembles into a liposome with an octanol pocket attached to it upon production. The octanol pocket later pinches off within a few minutes, resulting in a liposome and a separated octanol droplet.

We have previously presented an optofluidic permeability assay which allows us to determine the permeability coefficient of electroformed GUVs to fluoroquinolone drugs in a direct, label-free manner.[18] The assay exploits the autofluorescence property of fluoroquinolones in the ultraviolet region for label-free detection. GUVs are exposed to a drug solute in a controlled manner in a microfluidic device. We use ultraviolet video fluorescence microscopy to quantify drug uptake in the GUVs and report the permeability coefficient of the drug across the membrane composition of interest. We used this method to show the influence of lipid composition on fluoroquinolone transport.[19] Furthermore, we showed that the permeability of different drugs from the fluoroquinolone family can span over 2 orders of magnitude at different pH levels.[20] Finally, we used the assay to study the transport behavior of proteoliposomes containing the *E. coli* outer membrane protein OmpF,[21] thus developing a direct, optical measurement for antibiotic flux through porins, which form an important route for drug molecules to translocate across the outer membrane of Gram-negative bacteria.[5]

Despite these advances, the technique suffered from the various drawbacks of off-chip liposome formation described above. In this paper, we present the successful integration of the OLA platform with our optofluidic transport assay. This lab-on-chip total analysis platform enables the continuous production and screening of liposomes on the same device. This enabled us to efficiently screen an order of magnitude more liposomes than in our earlier platform. Importantly, it also enables us to explore transport using physiological salt concentrations, which was challenging using electroformed GUVs.[22] We also present an improved MATLAB analysis routine, which offers superior liposome detection, automatic channel recognition, and more debugging options than our earlier platform. The method was validated by performing transport experiments of the fluoroquinolone drugs norfloxacin and ciprofloxacin through biomimetic PGPC liposomal membranes. We verified that the liposomes produced are indeed unilamellar by performing a dithionite bleaching assay.

2. MATERIALS AND METHODS

2.1. Microfluidic Chip Design. The microfluidic device integrates the channel features used for OLA with a downstream *T*-junction geometry to form a complete lab-on-chip system for the continuous production and screening of liposomes. A schematic of the device is shown in Figure 1A.

The six-way junction where the liposomes are created is shown in Figure 2A. The design of the junction enables the formation of double emulsion droplets. This leads to the production of a lipid bilayer encapsulating an aqueous compartment with a 1-octanol pocket attached to it. The octanol droplet then buds off the liposome because of a

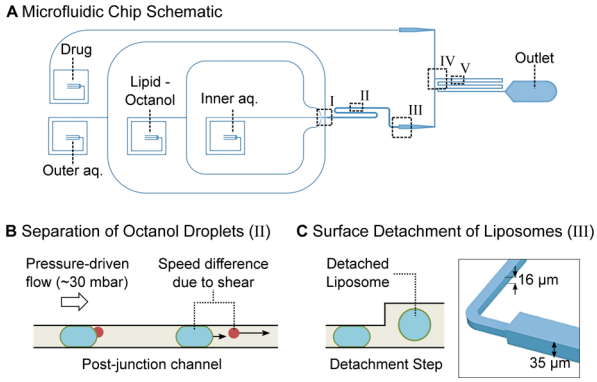

Figure 1. Microfluidic total analysis system for quantifying drug permeability across liposome membranes. (A) The microfluidic chip features four inlets, one outlet, and two different channel heights. The outer aqueous (OA), inner aqueous (IA), and lipid-octanol (LO) inlets are needed for liposome production on chip. The fourth inlet is used to flush in the drug whose permeability is to be measured. The liposome production occurs at a six-way junction, where the aqueous flows meet the LO phase (I). The 1-octanol pocket which is initially attached to the liposome separates from it in the post-junction channel within minutes after production (II). After an increase in channel height (III), the liposomes are mixed with the drug solute (IV). The transport measurement takes place as the liposomes flow toward the outlet, immersed in a bath of the autofluorescing drug (V). (B) Mechanism to separate the liposome population from the octanol droplets. The liposomes typically have radii of 15−18 μm upon production and octanol droplets of <8 μm. The channel height post formation is lower than the diameter of the liposomes, which leads to a significant difference in velocity for octanol droplets and liposomes as indicated by the arrows. The octanol droplets pass through the device first and are discarded at the outlet. (C) Upon production, the liposomes' diameters are larger than the height of the microfluidic channel. An increase in channel height from 16 to 35 μm frees the liposomes from the geometric confinement and enables transport measurements across the membrane without the risk of shear-induced leakage.

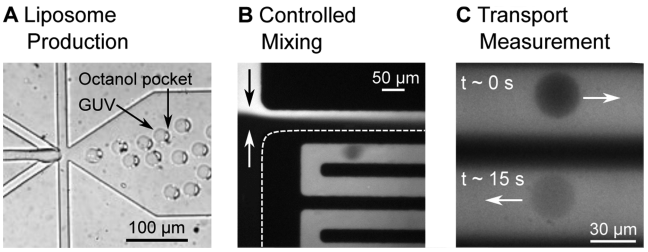

Figure 2. Liposomes at different positions in the microfluidic chip. (A) Liposome assembly at the six-way formation junction. A 1-octanol pocket is initially attached to the liposomes. The liposome and the octanol pocket separate further downstream in the post-junction channel. (B) Liposomes experience a spontaneous exposure to a drug solute at a *T*-junction where the two flows mix in a controlled manner. (C) Liposomes, surrounded by the autofluorescing drug (λ_{ex} = 350 nm), can be monitored at different parts of the channel, corresponding to different times that the liposome has been exposed to the drug. The increase in liposome intensity as the fluorescing drug diffuses across the membrane is used to determine the permeability coefficient of the drug across the lipid membrane under investigation.

combined effect of surface energy minimization and shear stress induced by the surrounding fluid streams, as well as contact with the channel wall.[17] The original design

DOI: 10.1021/acs.molpharmaceut.9b00086
Mol. Pharmaceutics 2019, 16, 2494−2501

geometry[17] was modified to fit the needs of the drug transport assay. The dimensions of the junction were scaled up by a factor of 2 to achieve liposome diameters of up to 35 μm. The larger channels furthermore lead to higher flow rates and higher liposome production rates. A side effect of the larger liposomes and the altered flow conditions is that the budding off of the octanol pocket from the liposomes requires more time than for smaller vesicles. The budding-off process has previously been reported to occur within a minute after production,[23] whereas this process is on the time scale of minutes using our chip geometry.

The generated liposomes have diameters larger than the height of the post-junction channel. These liposomes therefore initially shear along the polydimethylsiloxane (PDMS) walls, as they flow downstream. To ensure that the shear does not compromise the membranes during the subsequent transport measurements, the channel height was increased from 16 to 35 μm (Figure 1C). After this, the liposomes flow toward the mixing junction without shearing.

Reaching the *T*-junction, the liposomes are exposed to a drug solute as they flow toward the outlet channel (Figure 2B). Drug transport across the liposome membrane is tracked label-free by exploiting the autofluorescence of the drug in the UV region (λ_{ex} = 350 nm). The liposomes initially appear dark on a bright background because of the lack of fluorescent drug molecules within them. As the fluorescent drug molecules diffuse through the membrane, the liposomes get brighter, as seen in Figure 2C. We record and analyze the increase in fluorescence intensity using a previously established analytical protocol to quantify the permeability coefficient of the drug molecule for the specific lipid composition under investigation.[18,20]

2.2. Separation of Octanol Droplets and Liposomes Based on Flow Speed. The shearing of the liposomes in the post-junction channel is exploited to separate the liposome population from the octanol droplets. This separation mechanism, visualized in Figure 1B, is based on the difference in flow speeds between the liposomes and the droplets. Upon production, the liposomes typically have radii of 15−18 μm, whereas the octanol droplets have radii less than 8 μm. The channel height of 16 μm before the step causes deformation and shearing of the liposomes with the PDMS and slows their flow speed down considerably. In comparison, the smaller octanol droplets do not shear and therefore possess a higher velocity. Liposomes typically move with speeds of ∼0.05 mm/s, whereas the droplets move at ∼0.2 mm/s in this region of the chip. We fill the post-formation channel with the required number of liposomes and subsequently terminate liposome formation by reducing the aqueous flows (IA and OA) and stopping the LO flow completely. The smaller octanol droplets in the channel get flushed through the mixing junction and out of the chip before the larger liposomes reach the junction; the process is possible because the surface interactions result in different flow speeds of the liposomes and smaller octanol droplets (Figure 1B). The velocity difference explains the observed separation of the octanol droplets and liposomes on chip. After reaching the step, the liposomes are no longer pressed against the channel walls, reconfigure to an expected isotropic spherical geometry, and encounter the drug flow at the *T*-junction.

2.3. Chip Fabrication. The microfluidic chips are made of PDMS using established photolithography and soft lithography techniques. The master mold is generated by spin-coating a thin layer of SU-8 2025 photoresist (Chestech, UK) on a 4 in. silicon wafer (University Wafer, USA). The wafer is prebaked on a hot plate at 65 °C for 1 min and at 95 °C for 6 min. The structures are imprinted on the substrate using a table-top laser direct imaging (LDI) system (LPKF ProtoLaser LDI, Germany). The LDI system exposes the structures specified in the software directly with UV light, causing the photoresist to cross-link and solidify. After exposure, the wafer is post-baked for 1 min at 65 °C and for 6 min at 95 °C. The substrate is developed by rinsing the wafer with propylene glycol monomethyl ether acetate, which removes the unexposed photoresist and leaves the desired UV-exposed structures on the substrate. The wafer is then hard-baked for 15 min at 120 °C. The multi-height feature is achieved by performing this photolithography process twice on the same silicon wafer with different layers of photoresist with varying heights. Feature heights of 16 and 35 μm were obtained by spinning the photoresist at 3800 and 1800 rpm, respectively (WS-650-23NPP, Laurell Technologies, USA) for 60 s with a ramp of 100 rpm/s. The anchoring tool of the direct laser writer is used for aligning the features in the two designs.

The PDMS microfluidic devices are made by using the silicon master as a mold. Liquid PDMS (Sylgard 184, Dow Corning) is mixed in a 9:1 ratio with the curing agent and desiccated to remove air bubbles. It is then cast into the mold and cured for 60 min at 60 °C. Fluid access ports of 0.75 mm diameter for the inlets and 1.5 mm diameter for the outlet are punched into the chip using biopsy punches (WPI, UK). The PDMS chip is then plasma-bonded to PDMS-coated cover slips using a standard plasma bonding protocol (100 W, 10 s exposure, 25 sccm, plasma oven from Diener Electric, Germany).

The surfaces of the outlet channel are rendered hydrophilic by flushing the channel with a polyvinyl alcohol (PVA) solution for 15 min (50 mg/mL, 87−90% hydrolyzed molecular weight 30 000−70 000 Da, Sigma-Aldrich) via the OA inlet, using a previously established protocol.[17] Post treatment, PVA is removed from the channels by applying suction with a vacuum pump (Gardner Denver Thomas GmbH, Germany) after which the microfluidic device is baked in the oven at 120 °C for 15 min.

2.4. Optical Setup. The microfluidic chips are either run on a custom-built UV epifluorescence setup or on a commercial epifluorescence microscope (Nikon TE 2000U) to induce autofluorescence in the drug molecules and to capture the experimental video data. In the custom-built setup, white light from a broadband light source (EQ99FC, Energetiq, USA) enters a monochromator (Monoscan 2000, Ocean Optics, USA) where the excitation wavelength (λ_{ex} = 350 nm) for the target drug molecule is selected. The UV light passes through a Köhler illumination pathway and illuminates the microfluidic device via a quad band dichroic mirror (BrightLine full-multiband filter set, Semrock, USA) and a microscope objective. The fluorescence signal is detected by an EMCCD camera (Evolve 512 Delta, Photometrics). The camera and recording settings (exposure 10 ms, bin 2, gain 150) are controlled using the open source software μManager 1.4.[24] A 60× water immersion objective (UPLSAPO NA 1.2, Olympus) is used for data recording, whereas lower magnifications (4×, 10×, 20×, Plan Achromat, Olympus) are used for optimizing the vesicle formation and PVA treatment of the chip. The Nikon epifluorescence microscope is equipped with a pE-1 LED lamp (λ_{ex} = 365 nm (DAPI), Cool LED, UK)

DOI: 10.1021/acs.molpharmaceut.9b00086
Mol. Pharmaceutics 2019, 16, 2494−2501

and uses the same water immersion objective, dichroic mirror, and camera (exposure 15 ms, bin 2, gain 250) as the custom-built setup.

2.5. Solution Compositions and Flow Control. The base solutions for the OLA aqueous phases consist of 200 mM sucrose and 15% v/v glycerol in buffer. In accordance with previously published protocols, the OA phase additionally contains 50 mg/mL of poloxamer Kolliphor P-188, which facilitates the initial double emulsion formation.[23] We performed experiments on the fluoroquinolone drugs norfloxacin and ciprofloxacin. Transport of both drugs is measured in phosphate-buffered saline (PBS; pH 7.4), which mimics physiological pH and salt concentrations. Additionally, experiments using a 5 mM acetic acid buffer (pH 5) are performed for norfloxacin as controls for membrane stability. At pH 5, norfloxacin molecules are primarily in their positively charged form and hence show low permeability through lipid bilayers.[18,20] The drug solutes are prepared by diluting 48.5 mM norfloxacin and 49.5 mM ciprofloxacin stock solutions, respectively, to a final concentration of 2 mM with the aqueous base stock. All pH levels are adjusted and checked using a digital pH meter (Hanna Instruments, UK). The LO phase is obtained by dissolving a 100 mg/mL lipid stock mixture with 1-octanol to reach a final concentration of 2 mg/mL. The lipid stock is a 3:1 mixture of 1,2-dioleoyl-*sn*-glycero-3-phosphocholine (DOPC) and 1,2-dioleoyl-*sn*-glycero-3-phospho-*rac*-(1-glycerol)sodium salt (DOPG) in 100% ethanol. DOPG is an anionic lipid with a net charge of −1. Lipid mixtures of DOPG with the net-charge neutral lipid DOPC roughly mimic the negative charge density of bacterial lipid extracts and are typically used when modeling bacterial membranes with GUVs.[25−28] All chemicals are obtained from Sigma-Aldrich, unless stated otherwise.

The liquid flows in the microfluidic device are controlled with a pressure-driven microfluidic pump (MFCS-EZ, Fluigent). The fluids are stored in Fluiwell-4C reservoirs (Micrewtube 0.5 mL, Simport) and enter the microfluidic chip via a polymer tubing (Tygon microbore tubing, 0.020″ × 0.060″ OD, Cole Parmer). Cut dispensing tips (Gauge 23 blunt end, Intertronics) are used as metal connectors between the tubing and the chip.

2.6. Experimental Protocol. The microfluidic assay involves a two-stage protocol. The first stage involves adjusting the pressure-driven flows of the liquids to obtain stable liposome production, as reported previously.[17] Typically, pressures of ∼40 mbar for the IA, LO, and drug inlet phases and ∼70 mbar for the OA phases lead to a stable production of liposomes. After the post-formation channel has been typically filled with hundreds of liposomes, the aqueous flows are reduced (IA and OA input pressures at this stage are typically reduced to around 15 mbar each), and the LO flow is stopped completely. Because of the difference in flow speeds described in Figure 1B, the octanol droplets flow out of the chip leaving a population of octanol-free liposomes in the post-formation channel. Throughout the entire process, the *T*-junction is regularly monitored to ensure that the drug and OLA flows mix equally and that no octanol enters the drug channel.

The next stage involves the drug permeability measurement, using the same measurement principles previously employed in our laboratory.[18−21] The field-of-view is changed to the channel network post the *T*-junction, shortly after the liposomes encounter the drug flow (Figure 2C). Using a 60× water immersion objective (UPLSAPO, NA 1.2, Olympus), two sections of the channel are monitored simultaneously with sufficient resolution to study the transport process. Because the liposome is dispensed in the drug solution flowing along the channel, the different positions in the channel correspond to different drug exposure times of the liposome. The IA and OA pressures are maintained at 15 mbar each, resulting in flow speeds in the channel of about 0.5 mm/s. One measurement is taken just after the drug and the vesicle flows meet ($t \approx 0$ s) and the other one typically after the liposomes have been exposed to the drug for ∼15 s. Measurements of up to 40 s of drug exposure can be obtained at these flow rates by recording the liposomes at the end of the channel network, just before the outlet reservoir. This can be further increased by increasing the length of the mixing channel.[18]

After all the liposomes have been flushed through, the liposome formation can be restarted, and the experiment can be repeated. The number of repeats is limited by the quality of the PVA coating and/or accumulation of lipid and octanol aggregates in the chip. The data presented here were obtained by performing up to four such repeats on a single chip. However, more repeats are possible, and we managed to use a chip to perform up to 11 experiments consecutively. Generally, OLA allows for continuous liposome production with a frequency of up to 100 Hz for several hours.[23]

2.7. Data Processing and Permeability Calculation. The data are analyzed using our previously established permeability model.[18−20] The videos obtained are processed using a MATLAB routine. Similar to our previously reported analysis routine, the script extracts the radius, the speed, the circularity, and the intensity values of the liposomes passing through the channels. We have updated the image analysis routine, which now additionally features superior liposome detection, automatic channel recognition, and debugging options that are explained in detail in the Supporting Information.

The permeability coefficient is obtained by the equation[18]

$$P = -\left(\frac{R}{3t}\right) \times \ln(\Delta I(t) - \Delta I(0) + 1)$$

where the variable R is the radius of the liposome, t is the time of its exposure to the antibiotic, and ΔI is the normalized autofluorescence intensity difference between the interior (I_{in}) and the exterior (I_{out}) of the liposome

$$\Delta I = \frac{I_{out} - I_{in}}{I_{out}}$$

The difference in the normalized intensity of the liposomes at different drug exposure times can be used as a direct readout of drug flux into the liposomes.[18] Because of the initial lack of fluorescing drug molecules inside the liposome, $\Delta I(t = 0)$ has a high value, correlating to a large difference in fluorescence intensity between the liposome (I_{in}) and the background (I_{out}). In contrast, $\Delta I(t)$ at the later time point has a lower value consistent to a lower difference in fluorescence intensity between the liposome and the background because of the influx of fluorescing drug molecules. Further explanations and a derivation of the equations have been published in our previous work.[18,20]

DOI: 10.1021/acs.molpharmaceut.9b00086
Mol. Pharmaceutics 2019, 16, 2494−2501

3. RESULTS

3.1. Test for Membrane Unilamellarity. Liposomes produced by OLA have previously been tested for their unilamellarity via the incorporation of the pore-forming toxin α-hemolysin.[17] Additionally, the antimicrobial peptide cecropin B was found to permeabilize and lyse OLA-produced liposomes, again suggesting that the liposomes are unilamellar.[28] As an additional, quantitative technique to verify the unilamellarity of the OLA-produced liposomes, we extracted the liposomes from our microfluidic device and subjected them to a dithionite bleaching assay. If brought in contact with it, the membrane-impermeable anion dithionite reduces and thereby irreversibly bleaches nitrobenzoxadiazole (NBD). By subjecting unilamellar liposomes containing NBD-labeled lipids to a dithionite solution, the fluorescence intensity of the liposome drops to half of the initial value because of the bleaching of the outer leaflet of the bilayer membrane.[29,30]

The composition of the IA and OA solutions used for liposome production in this experiment is identical to the solutions of the drug transport assay described above. The LO phase additionally contains 0.01 mg/mL of a fluorescently labeled NBD-PC lipid (1-palmitoyl-2-{6-[(7-nitro-2-1,3-benzoxadiazol-4-yl)amino]hexanoyl}-*sn*-glycero-3-phosphocholine, Avanti Polar Lipids, USA). A standard PDMS chip with the design shown in Figure 1 is used to extract the liposomes off chip. However, instead of applying a Ø 1.5 mm punch at the outlet, a Ø 4 mm hole is punched at the detachment step in this case. The Ø 4 mm outlet serves as a fluid reservoir where the liposomes are collected. After the pressures of the microfluidic pump have been adjusted to achieve a stable liposome production, an additional 20 μL of the IA solution is pipetted into the reservoir, which aids the separation of liposomes and octanol droplets in the reservoir. Because of the lower density of octanol, the droplets rise to the surface of the reservoir. A larger fluid volume furthermore facilitates liposome extraction. After 1 h of liposome production, 15 μL of the liposome suspension is extracted from the reservoir using a wide bore pipette tip.

The liposome suspension is added to a microscopy chamber (Grace Bio-Labs FlexWell, Sigma-Aldrich) on a bovine serum albumin-coated coverslip containing 35 μL of a solution containing PBS, 200 mM glucose, and 15% v/v glycerol. The liposomes are left for 1 h to sink and settle at the bottom of the chamber, which facilitates imaging. A dithionite solution stock (1 M sodium dithionite in Tris pH 10 buffer, Sigma-Aldrich) is diluted in the glucose buffer to a final dithionite concentration of 15 mM. The solution (30 μL) is added to the liposome suspension after the imaging is started.[30] Imaging is performed on a confocal microscope (Olympus IX83, FV10-MCPSU laser system, 20× objective UPLSAPO Olympus, 5 s frame interval). Image analysis is performed using the open source software Image J.

The intensity traces of the liposomes normalized to their initial intensity value are depicted in Figure 3. Figure 3A shows the intensity drop upon addition of dithionite, whereas Figure 3B shows the results of the bleaching control experiment upon addition of buffer without dithionite. The mean intensity of the observed liposomes is shown as black line with the standard deviations depicted in gray. The intensity of the liposomes subjected to dithionite (N = 10) drops to half of the initial intensity after about 500 s and then remains steady at that value. These results suggest that the liposomes indeed consist

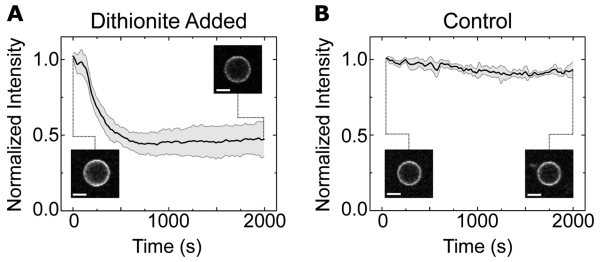

Figure 3. Normalized intensity traces of the liposome membranes. (A) Intensity drop of the liposome membranes (N = 10) upon addition of dithionite. The mean intensity of the observed liposomes is shown in black with the standard deviations depicted in gray. The drop to half of the initial value is caused by the bleaching of the outer membrane leaflet by the dithionite. (B) Liposome intensity (N = 3) remains stable throughout the entire experiment upon addition of buffer without dithionite, suggesting a negligible effect of photobleaching. The insets show a representative liposome at the beginning of the measurement and after 2000 s. The scale bars show 10 μm.

of a single lipid bilayer, whose outer leaflet is bleached by the dithionite.[29] Because the dithionite anion cannot penetrate the membrane, the inner leaflet of the membrane is not affected by the dithionite and remains fluorescent. The control experiment without dithionite in Figure 3B shows a stable intensity signal over the time span of the entire experiment (N = 3). This suggests that photobleaching does not play a significant role in the observed drop in the intensity and that we are indeed observing the bleaching of the outer leaflet of a single bilayer.

3.2. Passive Diffusion Measurements. Norfloxacin transport measurements were performed in two different chemical environments. One set of measurements was performed at physiological pH and salt concentrations (PBS). The second set was taken as a control in an acetic acid buffer at pH 5. The majority of norfloxacin molecules are positively charged at pH 5, whereas the proportion of uncharged molecules is increased at pH 7.4.[18,20,21,31] The liposomes consisted of PCPG lipids in a 3:1 ratio, a mixture which is commonly used as a model for bacterial membranes because of its negative charge.[25,26]

The scatter plots in Figure 4 show representative results from such experiments. The black data points mark the normalized intensity difference levels $\Delta I(0)$ of individual

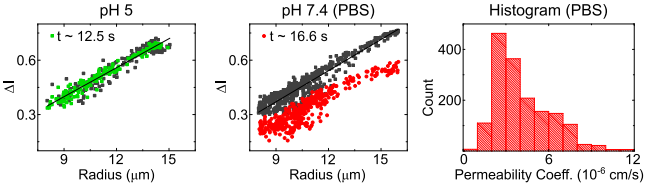

Figure 4. Norfloxacin diffusion experiments across PCPG liposomal membranes. The scatter plots show representative drug uptake experiments at pH 5 and pH 7.4. Each point in the scatter plots corresponds to the measured normalized intensity difference of a liposome. The dark points are obtained at $t \approx 0$, just after the liposomes encounter the drug flow. The colored points show the value at the second measurement position, after exposure to the drug for the time indicated in the panel. The gap between the black and red points for the measurement in PBS indicates norfloxacin membrane permeability. The histogram shows the distribution of all permeability measurements combined at pH 7.4 (N = 1620, 5 technical repeats). The distribution has a mean value of $4.13 \pm 0.05 \times 10^{-6}$ cm/s (mean ± std. error of mean) and a median value of 3.57×10^{-6} cm/s.

DOI: 10.1021/acs.molpharmaceut.9b00086
Mol. Pharmaceutics 2019, 16, 2494−2501

liposomes at the first measurement point, when the liposomes have just encountered the drug flow and hence do not contain any drug molecules within them. The colored data points mark the normalized intensity difference $\Delta I(t)$ of the individual liposomes after they have been exposed to the drug for the time indicated inset. The liposomes in PBS show a substantial drop in ΔI after being exposed to the drug, whereas the measurements at the different time points overlap when the studies are conducted at pH 5.

Because the drop in ΔI is a direct result of the influx of fluorescent molecules, we can conclude that no significant transport occurs at pH 5 over the observed time spans, whereas there is substantial norfloxacin transport at physiological pH and salt concentrations. The technical repeats of this experiment shown in Figures S3 and S4 (Supporting Information) report similar results. Expanding the exposure and observation time for the pH 5 measurement to 40 s yields the same result of no significant transport, in line with our previous observations. This also confirms that the liposome membranes are not being compromised because of shear or any other interactions in our device.

The observed transport behavior is to be expected, as the norfloxacin molecule is predominantly uncharged or zwitterionic at neutral pH, whereas the molecule is in a charged state at pH 5.[32] Lipid membranes are generally regarded as largely impermeable to ions and highly charged molecules because these cannot cross the hydrocarbon section of the lipid bilayer easily. In nature, these transport processes are governed by transmembrane proteins such as porins or ion channels.[33]

The spread in vesicle radius observed in Figure 4 is a result of the method used to separate the liposomes from the octanol droplet population. As illustrated in Figure 1B, the mechanism is based on a difference in flow velocity in the channel because of shearing of the liposomes. Throughout their travel to the step in channel height, the membranes are susceptible to small disruptions because of shear. The disruptions can lead to shrinking and separation of the liposomes. This spread in liposome size is illustrated in Figure S2 (Supporting Information). The gradient of the curve that the scatter points lie on is a result of the fact that our optical measurement is not a confocal measurement. The fluorescent drug solute surrounding smaller liposomes therefore leads to a lower apparent ΔI, compared to larger liposomes (for a detailed explanation, refer to Cama et al.[18,20]). The analysis protocols are hence identical to our previously established technique.

The resulting permeability coefficients of all the norfloxacin experiments performed in PBS are combined in the histogram in Figure 4. The total number of liposomes in the histogram is 1620 and results in an overall average permeability coefficient of $4.13 \pm 0.05 \times 10^{-6}$ cm/s (mean ± std. error of mean) and a median value of 3.57×10^{-6} cm/s. The values were obtained from 12 experiments in five technical repeats. For the pH 5 measurement, five experiments on two technical repeats were performed. An experiment is defined as a continuously acquired dataset measured from one batch of liposomes produced on the microfluidic device. As described above, up to four experiments were performed on one microfluidic device by restarting the liposome production after completion of one measurement. Each set of experiments performed on an individual device is defined as a technical repeat.

The value obtained from the transport measurements matches the values previously obtained in our group using the established electroformation liposome production technique. Purushothaman et al. measured the permeability coefficient of norfloxacin through PGPC liposomes (30:70 ratio) in a 5 mM phosphate buffer solution at pH 7.0 to be $4.3 \pm 0.2 \times 10^{-6}$ cm/s.[19] The main advantages of the on-chip OLA technique over electroformation are the high-throughput liposome production and its compatibility with physiological salt concentrations. The higher liposome production efficiency allows us to perform tests on 1620 liposomes here compared to the 138 liposomes in previous experiments using electroformation. Because of the greater efficiency of vesicle formation under these conditions and the correspondingly higher number of data points, we can provide a more precise estimate of the permeability coefficient than before, with the standard error of the mean lowered by over an order of magnitude compared to the results previously reported[19] using electroformed vesicles. Furthermore, the possibility of producing liposomes at physiological salt concentrations allows us to mimic the natural environment of a bacterial cell more closely. Any possible remaining traces of solvent[23] (1-octanol, poloxamer P-188) do not seem to alter the transport properties of the membrane, as seen by the similarity to the previously acquired result.

The scatter plots and histogram of the permeability measurements for ciprofloxacin are displayed in Figure S5 (Supporting Information). The mean (±std. error of mean) permeability coefficient obtained for this drug is $4.99 \pm 0.07 \times 10^{-6}$ cm/s, and the median value is 4.8×10^{-6} cm/s. The values are obtained from 4 experiments (4 technical repeats) and a total of 960 vesicles. The higher permeability coefficient of ciprofloxacin compared with norfloxacin is to be expected based on the chemical structure of the respective molecules. Norfloxacin carries an ethyl group at the $N-1$ position, where ciprofloxacin has a cyclopropyl group. This functional group is associated with higher lipophilicity of the compound and therefore results in a higher permeability coefficient.[20]

4. DISCUSSION AND CONCLUSIONS

In this paper, we presented an integrated microfluidic platform for quantifying drug permeation across biomimetic membranes. We combined an on-chip liposome formation technique (OLA) with a downstream *T*-junction for the controlled exposure of liposomes to a drug solute. Norfloxacin and ciprofloxacin transport through biomimetic PGPC (1:3 ratio) liposomes was measured at physiological pH and salt concentrations. The measurements yielded permeability coefficients of $4.13 \pm 0.05 \times 10^{-6}$ cm/s (mean ± std. error of mean) with a median value of 3.57×10^{-6} cm/s for norfloxacin and $4.99 \pm 0.07 \times 10^{-6}$ cm/s (mean ± std. error of mean) and a median value of 4.8×10^{-6} cm/s for ciprofloxacin. These values are in good agreement with previous measurements.[19,20] We produced PGPC (1:3) liposomes to mimic the anionic charge density typically associated with bacterial membranes[25−28] and used this as a model system to quantify passive drug transport through the lipid bilayer component of the Gram-negative cell envelope.

Because our method directly quantifies the permeability coefficient of the drug across the specific membrane of interest, our technique offers an alternative to traditional drug transport assays such as octanol partition coefficients or the parallel artificial membrane permeability assay, which suffer from multiple drawbacks.[34,35] Our method also profits from recent advances in the development of fluorescent antibiotics, as these provide another potential tool for studying and understanding

DOI: 10.1021/acs.molpharmaceut.9b00086
Mol. Pharmaceutics 2019, 16, 2494−2501

drug transport processes that will lead to further insight into drug−membrane interactions.[36] Importantly, thanks to the microfluidic character of our method, we require only very small reagent volumes in the microliter range for our measurements.[37]

Another advantage of the integrated on-chip technique presented here over our previously published optofluidic permeability assay lies in the benefits of controlling liposome formation with OLA. OLA allows the formation of large numbers of liposomes with physiological salt concentrations and with complex lipid mixtures. Other techniques such as electroformation suffer from very low yields in this environment[15] or in the case of other microfluidic techniques require extensive procedures to remove oil remnants associated with the production.[17] Moreover, OLA allows for the efficient encapsulation of desired solutes inside the vesicles upon production.[17,27] This makes it an interesting technique for biosensor-based approaches to detect drug molecules. The encapsulation approach has successfully been performed by Kuhn et al. to measure tetracycline transport across lipid bilayers.[38] However, their experiments were performed using populations of small unilamellar vesicles of under 200 nm in radius, whereas we can work with GUVs and analyze drug transport on the single vesicle level.

Furthermore, the microfluidic platform presented here is not bound to a specific form of visualization such as fluorescence. Because the optics and the microfluidics are decoupled from one another, the platform can be combined with different approaches of label-free drug visualization, which is a field in its own right with various different methods published.[39−42] Our platform may offer the opportunity to study nonfluorescent molecules in the future.

While passive diffusion across lipids is an important element in bacterial drug uptake, it is known that porin-mediated uptake plays a crucial role in drug permeation across the outer membrane.[7,21] Mutations of membrane proteins have furthermore been associated with antibiotic resistance.[21,43] The incorporation of these protein channels into liposomal membranes is an attractive target for the study of drug uptake.[7] However, to integrate this with on-chip liposome formation requires the development of on-chip protein reconstitution techniques, which are still pending. The successful insertion of the pore-forming toxin α-hemolysin into the membrane of OLA-generated liposomes[17] suggests that the microfluidic platform can be extended to form and study more complex lipid compositions and even proteoliposomes on chip, potentially offering an alternative to current reconstitution techniques.[44]

■ ASSOCIATED CONTENT

Supporting Information

The Supporting Information is available free of charge on the ACS Publications website at DOI: 10.1021/acs.molpharmaceut.9b00086.

Complete experimental data set, details on the MATLAB analysis, and spread of liposome radius (PDF)

■ AUTHOR INFORMATION

Corresponding Author

*E-mail: ufk20@cam.ac.uk.

ORCID

Michael Schaich: 0000-0001-5432-9598
Jehangir Cama: 0000-0002-5982-1941
Kevin Jahnke: 0000-0001-7311-6993
Siddharth Deshpande: 0000-0002-7137-8962
Cees Dekker: 0000-0001-6273-071X

Notes

The authors declare no competing financial interest.

■ ACKNOWLEDGMENTS

M.S. is funded by the Friedrich-Naumann-Foundation for Freedom. J.C. acknowledges funding from the BBSRC, the ERC and from a Wellcome Trust Institutional Strategic Support Award to the University of Exeter (204909/Z/16/Z). K.A.N. acknowledges support from an EPSRC CASE award with the National Physical Laboratory, Winton Programme for the Physics of Sustainability, Trinity-Henry Barlow Scholarship, and the ERC. D.S. is funded by the Winton Programme for the Physics of Sustainability and the EPSRC. K.J. was supported by the Erasmus Plus student exchange programme. S.D. and C.D. acknowledge support from the ERC Advanced grants SynDiv (no. 669598) and the Netherlands Organisation for Scientific Research (NWO/OCW), as part of the Frontiers of Nanoscience program. U.F.K. acknowledges support from an ERC consolidator grant (Designer-Pores 647144).

■ REFERENCES

(1) McKenna, M. Antibiotic Resistance: The Last Resort. *Nature* **2013**, *499*, 394−396.
(2) ECDC2016. *ECDC: Surveillance Report. Surveillance of Antimicrobial Resistance in Europe 2016*: Stockholm, 2016.
(3) Blair, J. M. A.; Webber, M. A.; Baylay, A. J.; Ogbolu, D. O.; Piddock, L. J. V. Molecular Mechanisms of Antibiotic Resistance. *Nat. Rev. Microbiol.* **2015**, *13*, 42−51.
(4) Silver, L. L. A Gestalt Approach to Gram-Negative Entry. *Bioorg. Med. Chem.* **2016**, *24*, 6379−6389.
(5) Pagès, J.-M.; James, C. E.; Winterhalter, M. The Porin and the Permeating Antibiotic: A Selective Diffusion Barrier in Gram-Negative Bacteria. *Nat. Rev. Microbiol.* **2008**, *6*, 893−903.
(6) Six, D. A.; Krucker, T.; Leeds, J. A. Advances and Challenges in Bacterial Compound Accumulation Assays for Drug Discovery. *Curr. Opin. Chem. Biol.* **2018**, *44*, 9−15.
(7) Delcour, A. H. Outer Membrane Permeability and Antibiotic Resistance. *Biochim. Biophys. Acta—Proteins Proteomics* **2009**, *1794*, 808−816.
(8) Barák, I.; Muchová, K. The Role of Lipid Domains in Bacterial Cell Processes. *Int. J. Mol. Sci.* **2013**, *14*, 4050−4065.
(9) Fenz, S. F.; Sengupta, K. Giant Vesicles as Cell Models. *Integr. Biol.* **2012**, *4*, 982.
(10) Sercombe, L.; Veerati, T.; Moheimani, F.; Wu, S. Y.; Sood, A. K.; Hua, S. Advances and Challenges of Liposome Assisted Drug Delivery. *Front. Pharmacol.* **2015**, *6*, 286.
(11) Deshpande, S.; Spoelstra, W. K.; van Doorn, M.; Kerssemakers, J.; Dekker, C. Mechanical Division of Cell-Sized Liposomes. *ACS Nano* **2018**, *12*, 2560−2568.
(12) Xu, C.; Hu, S.; Chen, X. Artificial Cells: From Basic Science to Applications. *Mater. Today* **2016**, *19*, 516−532.
(13) Göpfrich, K.; Platzman, I.; Spatz, J. P. Mastering Complexity: Towards Bottom-up Construction of Multifunctional Eukaryotic Synthetic Cells. *Trends Biotechnol.* **2018**, *36*, 938−951.
(14) Akbarzadeh, A.; Rezaei-Sadabady, R.; Davaran, S.; Joo, S. W.; Zarghami, N.; Hanifehpour, Y.; Samiei, M.; Kouhi, M.; Nejati-Koshki, K. Liposome: Classification, Preparation, and Applications. *Nanoscale Res. Lett.* **2013**, *8*, 102.

DOI: 10.1021/acs.molpharmaceut.9b00086
Mol. Pharmaceutics 2019, 16, 2494−2501

(15) van Swaay, D.; DeMello, A. Microfluidic Methods for Forming Liposomes. *Lab Chip* **2013**, *13*, 752.
(16) Teh, S.-Y.; Khnouf, R.; Fan, H.; Lee, A. P. Stable, Biocompatible Lipid Vesicle Generation by Solvent Extraction-Based Droplet Microfluidics. *Biomicrofluidics* **2011**, *5*, 044113.
(17) Deshpande, S.; Caspi, Y.; Meijering, A. E. C.; Dekker, C. Octanol-Assisted Liposome Assembly on Chip. *Nat. Commun.* **2016**, *7*, 10447.
(18) Cama, J.; Chimerel, C.; Pagliara, S.; Javer, A.; Keyser, U. F. A Label-Free Microfluidic Assay to Quantitatively Study Antibiotic Diffusion through Lipid Membranes. *Lab Chip* **2014**, *14*, 2303−2308.
(19) Purushothaman, S.; Cama, J.; Keyser, U. F. Dependence of Norfloxacin Diffusion across Bilayers on Lipid Composition. *Soft Matter* **2016**, *12*, 2135−2144.
(20) Cama, J.; Schaich, M.; Al Nahas, K.; Hernández-Ainsa, S.; Pagliara, S.; Keyser, U. F. Direct Optofluidic Measurement of the Lipid Permeability of Fluoroquinolones. *Sci. Rep.* **2016**, *6*, 32824.
(21) Cama, J.; Bajaj, H.; Pagliara, S.; Maier, T.; Braun, Y.; Winterhalter, M.; Keyser, U. F. Quantification of Fluoroquinolone Uptake through the Outer Membrane Channel OmpF of Escherichia Coli. *J. Am. Chem. Soc.* **2015**, *137*, 13836−13843.
(22) Stein, H.; Spindler, S.; Bonakdar, N.; Wang, C.; Sandoghdar, V. Production of Isolated Giant Unilamellar Vesicles under High Salt Concentrations. *Front. Physiol.* **2017**, *8*, 63.
(23) Deshpande, S.; Dekker, C. On-Chip Microfluidic Production of Cell-Sized Liposomes. *Nat. Protoc.* **2018**, *13*, 856−874.
(24) Edelstein, A. D.; Tsuchida, M. A.; Amodaj, N.; Pinkard, H.; Vale, R. D.; Stuurman, N. Advanced methods of microscope control using μManager software. *J. Biol. Methods* **2014**, *1*, 10.
(25) Ryadnov, M. G.; Mukamolova, G. V.; Hawrani, A. S.; Spencer, J.; Platt, R. RE Coil: An Antimicrobial Peptide Regulator. *Angew. Chem., Int. Ed.* **2009**, *48*, 9676−9679.
(26) Vecchiarelli, A. G.; Li, M.; Mizuuchi, M.; Mizuuchi, K. Differential affinities of MinD and MinE to anionic phospholipid influence Min patterning dynamicsin vitro. *Mol. Microbiol.* **2014**, *93*, 453−463.
(27) Rakowska, P. D.; Jiang, H.; Ray, S.; Pyne, A.; Lamarre, B.; Carr, M.; Judge, P. J.; Ravi, J.; Gerling, U. I. M.; Koksch, B.; et al. Nanoscale Imaging Reveals Laterally Expanding Antimicrobial Pores in Lipid Bilayers. *Proc. Natl. Acad. Sci. U.S.A.* **2013**, *110*, 8918−8923.
(28) Al Nahas, K.; Cama, J.; Schaich, M.; Hammond, K.; Deshpande, S.; Dekker, C.; Ryadnov, M. G.; Keyser, U. F. A Microfluidic Platform for the Characterisation of Membrane Active Antimicrobials. *Lab Chip* **2019**, *19*, 837−844.
(29) McIntyre, J. C.; Sleight, R. G. Fluorescence Assay for Phospholipid Membrane Asymmetry. *Biochemistry* **1991**, *30*, 11819−11827.
(30) Ohmann, A.; Li, C.-Y.; Maffeo, C.; Al Nahas, K.; Baumann, K. N.; Göpfrich, K.; Yoo, J.; Keyser, U. F.; Aksimentiev, A. A Synthetic Enzyme Built from DNA Flips 10^7 Lipids per Second in Biological Membranes. *Nat. Commun.* **2018**, *9*, 2426.
(31) Nikaido, H.; Thanassi, D. G. Penetration of Lipophilic Agents with Multiple Protonation Sites into Bacterial Cells: Tetracyclines and Fluoroquinolones as Examples. *Antimicrob. Agents Chemother.* **1993**, *37*, 1393−1399.
(32) Uivarosi, V. Metal Complexes of Quinolone Antibiotics and Their Applications: An Update. *Molecules* **2013**, *18*, 11153−11197.
(33) Yang, N. J.; Hinner, M. J. Getting Across the Cell Membrane: An Overview for Small Molecules, Peptides, and Proteins. *Methods Mol. Biol.* **2015**, *1266*, 29−53.
(34) Avdeef, A.; Bendels, S.; Di, L. i.; Faller, B.; Kansy, M.; Sugano, K.; Yamauchi, Y. PAMPA-critical factors for better predictions of absorption. *J. Pharm. Sci.* **2007**, *96*, 2893−2909.
(35) Galinis-Luciani, D.; Nguyen, L.; Yazdanian, M. Is PAMPA a Useful Tool for Discovery? *J. Pharm. Sci.* **2007**, *96*, 2886−2892.
(36) Stone, M. R. L.; Butler, M. S.; Phetsang, W.; Cooper, M. A.; Blaskovich, M. A. T. Fluorescent Antibiotics: New Research Tools to Fight Antibiotic Resistance. *Trends Biotechnol.* **2018**, *36*, 523−536.
(37) Streets, A. M.; Huang, Y. Chip in a Lab: Microfluidics for next Generation Life Science Research. *Biomicrofluidics* **2013**, *7*, 011302.
(38) Kuhn, P.; Eyer, K.; Allner, S.; Lombardi, D.; Dittrich, P. S. A Microfluidic Vesicle Screening Platform: Monitoring the Lipid Membrane Permeability of Tetracyclines. *Anal. Chem.* **2011**, *83*, 8877−8885.
(39) Zeng, J.; Eckenrode, H. M.; Dounce, S. M.; Dai, H.-L. Time-Resolved Molecular Transport across Living Cell Membranes. *Biophys. J.* **2013**, *104*, 139−145.
(40) Nguyen, T. T.; Rembert, K.; Conboy, J. C. Label-Free Detection of Drug-Membrane Association Using Ultraviolet−Visible Sum-Frequency Generation. *J. Am. Chem. Soc.* **2009**, *131*, 1401−1403.
(41) Custódio, J. A.; Almeida, L. M.; Madeira, V. M. C. A Reliable and Rapid Procedure to Estimate Drug Partitioning in Biomembranes. *Biochem. Biophys. Res. Commun.* **1991**, *176*, 1079−1085.
(42) Fox, C. B.; Horton, R. A.; Harris, J. M. Detection of Drug−Membrane Interactions in Individual Phospholipid Vesicles by Confocal Raman Microscopy. *Anal. Chem.* **2006**, *78*, 4918−4924.
(43) Watanabe, T. Infective heredity of multiple drug resistance in bacteria. *Bacteriol. Rev.* **1963**, *27*, 87−115.
(44) Jørgensen, I. L.; Kemmer, G. C.; Pomorski, T. G. Membrane Protein Reconstitution into Giant Unilamellar Vesicles: A Review on Current Techniques. *Eur. Biophys. J.* **2017**, *46*, 103−119.

DOI: 10.1021/acs.molpharmaceut.9b00086
Mol. Pharmaceutics 2019, 16, 2494−2501